Ionization in Rydberg-atom—SF_6 collisions at high n

B. G. Zollars, C. Higgs,* F. Lu, C. W. Walter, L. G. Gray, K. A. Smith, F. B. Dunning, and R. F. Stebbings
Department of Space Physics and Astronomy and the Rice Quantum Institute, Rice University, Houston, Texas 77251
(Received 13 May 1985)

Absolute rate constants for ionization of Rb(ns,nd) atoms in collisions with SF_6 have been measured for values of n in the range 38—106. In addition, the kinematics of such reactions have been investigated using Xe(nf) atoms. The data confirm that collisions of Rydberg atoms with targets that attach free low-energy electrons are well described by the "essentially-free"-electron model. Analysis of the data shows that the cross section $\sigma(v)$ for electron attachment to SF_6 at very low electron energies ($\lesssim 10$ meV) is inversely proportional to the electron velocity v and, if v is expressed in cm sec^{-1}, is given by $\sigma(v)=(4.2\pm1.0)\times10^{-7}/v$ cm^2.

Ionization of atoms in Rydberg states through collisions with SF_6 has been studied by a number of workers.[1–5] These investigations show that, as confirmed in the present work, collisional ionization results predominantly from the electron transfer reaction

$$X^{**}+SF_6 \rightarrow X^+ + SF_6^- \quad (1)$$

in which the excited Rydberg electron attaches to the target SF_6 molecule. One motivation for these studies is to test the validity of the so-called "essentially-free"-electron model.[6] In this model it is assumed that the separation between the Rydberg electron and its associated ionic core is so large that both do not simultaneously interact with a collision partner. The collision is then analyzed by considering only the interaction between the Rydberg electron and the target. A prediction of this model is that the rate constant for reaction (1) will be equal to that for attachment, by SF_6, of free electrons having the same velocity distribution as the Rydberg electron. Since the average kinetic energy of a Rydberg electron is only a few milli-electron-volts, the model suggests that the study of Rydberg collisions can provide information on electron interactions in a very-low-energy regime that is virtually inaccessible using alternative techniques.

In the present work we have extended previous studies of reaction (1) to Rydberg states with much larger values of principal quantum number n up to 106. At this value of n the average kinetic energy of the Rydberg electron is only ~ 1.2 meV. The essentially-free-electron model should be particularly applicable at high n because the average separation between the Rydberg electron and its associated ionic core is large. Furthermore, because attachment will occur at large separations, interactions between the product ions should be minimal. This lack of interaction is confirmed in the present work by kinematic studies which show that, at high n, the product X^+ ions follow essentially the same trajectories as the initial Rydberg atoms. The measured rate constants are in agreement with those expected on the basis of the essentially-free-electron model and free-electron attachment cross sections obtained using swarm[7,8] and the threshold photoelectron spectroscopy by electron attachment[9,10] (TPSA) techniques. The data demonstrate that, for targets having large rate constants for attachment of free low-energy electrons, Rydberg-atom collision studies can be used to obtain information on electron attachment at very low electron energies.

Rate constants for reaction (1) were measured using Rb(ns) and Rb(nd) Rydberg atoms. The apparatus is shown schematically in Fig. 1. A collimated beam of rubidium atoms is produced by effusion from an oven operating at ~ 200 °C. The atoms are excited in zero electric field to a selected ns or nd state by two-photon excitation using the modulated output of a Coherent Radiation model 699-21 frequency-stabilized, single-mode ring dye laser. The dye employed is Rh6G. The laser and atom beams intersect at right angles, resulting in an effective Doppler width $\lesssim 50$ MHz. This permits highly state-selective excitation as is illustrated in Fig. 2, which shows the Rydberg-atom production observed as the laser is scanned over the frequency range corresponding to excitation of $47\,^2D_{3/2,5/2}$ and $49\,^2S_{1/2}$ states. A number of well-defined peaks are evident whose origin can be understood by reference to the schematic partial term diagram shown in the inset. Natural rubidium has two isotopes, ^{85}Rb and ^{87}Rb, each of which has a nonzero nuclear spin

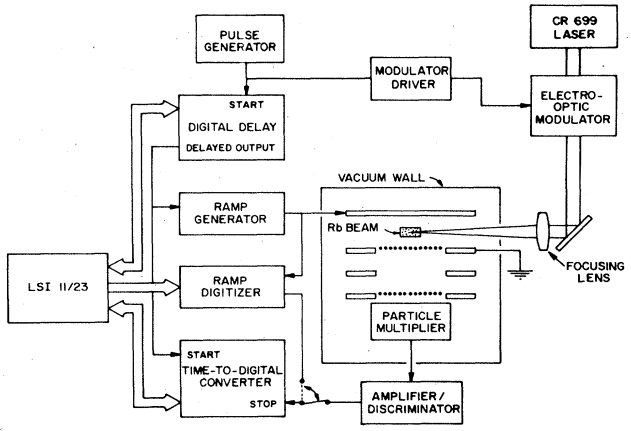

FIG. 1. Schematic diagram of the apparatus used to study Rb(ns,nd)-SF_6 collisions.

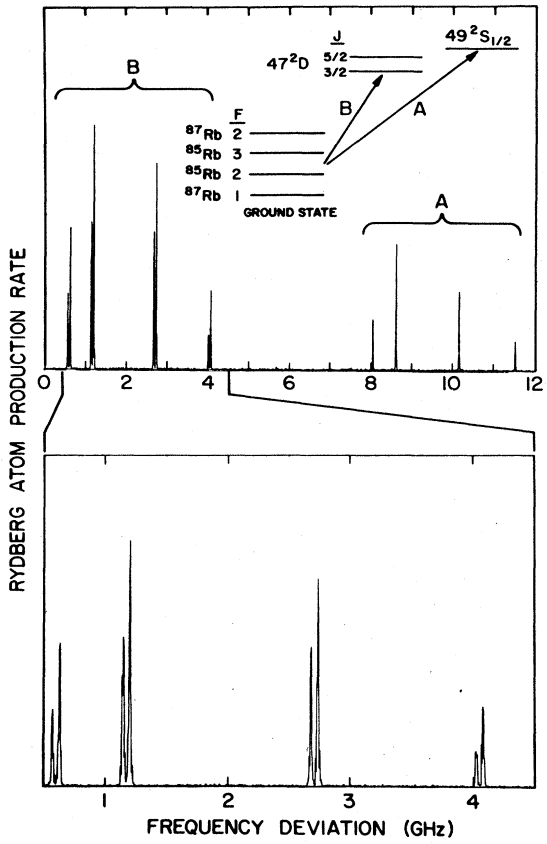

FIG. 2. Frequency dependence of Rydberg-atom production as the laser is scanned over the frequency interval corresponding to excitation of $47\,^2D_{3/2,5/2}$ and $49\,^2S_{1/2}$ states. The inset shows a partial term diagram for Rb.

and a large ground-state hyperfine splitting (3.036 GHz for ^{85}Rb, 6.835 GHz for ^{87}Rb).[11] The peaks labeled A result from transitions from the four resultant ground-state hyperfine levels to the $49\,^2S_{1/2}$ level. The peaks labeled B result from excitation to the $47\,^2D_{5/2}$ and $47\,^2D_{3/2}$ levels and, as is evident from the higher-resolution scan, transitions to these two fine-structure levels can be resolved. The present data were taken using $n\,^2D_{5/2}$ and $n\,^2S_{1/2}$ Rydberg states of ^{85}Rb. Values of n were determined by measuring the frequency separations between the S and D states and relating these to the accurately known n dependence of this quantity.[12,13] Data such as shown in Fig. 2 also demonstrate that excitation is occurring in very close to zero electric field because the presence of even a very small field leads to readily observable shifts and splitting of the nD levels.

In the present experiments the laser output is modulated using a fast Pockels cell to provide light pulses of 3 μsec width at a repetition frequency of $\sim$20 kHz. Excitation takes place, in the presence of target gas, near the center of an interaction region defined by two planar, parallel fine mesh grids. Following the laser pulse, collisions are allowed to occur for a selected time interval t. The total number of excited atoms remaining in the interaction region is then determined by selective field ionization (SFI). To accomplish this a pulsed electric field, which rises from zero to its maximum value in $\sim$500 nsec, is applied across the interaction region.[14,15] The electrons liberated by ionization are detected by a particle multiplier whose output is fed to a time to digital converter (TDC). The TDC is started at the beginning of the ionizing voltage ramp and is stopped by the first electron pulse subsequently registered by the detector. The output of the TDC is fed to an LSI 11/23 computer, which operates as a multichannel analyzer. For the present count rates, typically $\sim$100–500 Hz, the data stored in the computer give the probability of a field ionization event per unit time during the ionizing ramp. Measurement of the time dependence of the ionizing field strength[16] then permits the field dependence of the ionization signal to be determined. Since atoms in different Rydberg states ionize at different field strengths, analysis of SFI data yields the distribution of excited states present in the interaction region at the time the ionizing field is applied.

The SFI signal also provides a direct measure of the total number $N(t)$ of excited atoms present in the interaction region at time t after the laser pulse. The rate constant k for Rydberg-atom destruction is determined from measurements of the time dependence of $N(t)$, which for the present experimental conditions is given by

$$N(t)=N(0)e^{-bt}\,, \tag{2}$$

where

$$b=\frac{1}{\tau_{\text{eff}}}+\rho k$$

and $N(0)$ is the number of excited atoms present at the end of the excitation pulse, τ_{eff} is the effective radiative lifetime, and ρ is the target gas density, measured using an ion gauge calibrated against a capacitance manometer. Values of b were measured for several target gas densities. As expected, b was linearly dependent on target gas density and values of k were obtained directly from the slope of the b-ρ plot.

Analysis of the SFI profiles shows that collisions also result in state changing via reactions of the type

$$\text{Rb}(ns,nd)+\text{SF}_6\rightarrow\text{Rb}(n'l')+\text{SF}_6\,. \tag{3}$$

However, state-changing collisions do not lead to collisional destruction because the product atoms still contribute to the measured excited-state population $N(t)$. Collisional data were recorded at early times, typically 1–10 μsec after laser excitation, and at low target gas densities, typically $\lesssim 10^{11}$ cm^{-3}. This ensured that during the course of a measurement almost all atoms remained in the parent ns or nd state.

Earlier measurements in this laboratory showed that destruction of Rydberg atoms in collisions with SF_6 results predominantly from collisional ionization.[1,5,17] This was further confirmed in the present work by measuring rate constants for collisional ionization from direct observations of the time development of the product Rb^+-ion signal using a technique similar to that described elsewhere.[1] The rate constants so obtained are in good agreement with

TABLE I. Measured rate constants k. Also included for each n are the average kinetic energy $\bar{\epsilon}$ of the Rydberg electron and the Rydberg electron attachment cross section σ_e as defined in Eq. (5).

Parent state	k (10^{-7} cm^{3}sec^{-1})	σ_e (10^{-14} cm^2)	$\bar{\epsilon}$ (meV)
38D	4.8±1.0	8.0±1.6	10.1
41D	4.4±1.1	8.1±2.0	8.7
41D[a]	3.9±1.0	7.1±1.8	8.7
44D	4.4±1.1	8.5±2.1	7.5
47D	4.6±0.9	9.5±1.9	6.5
49S	5.1±1.1	10.8±2.2	6.5
50D	4.3±0.9	9.6±1.9	5.8
54D	4.4±1.1	10.6±2.7	4.9
54D[a]	3.7±0.9	9.0±2.2	4.9
56S	3.8±0.8	9.2±1.8	4.9
59D	4.0±1.0	10.6±2.7	4.1
61D	4.0±1.0	10.9±2.7	3.8
61S	3.9±1.0	10.2±2.6	4.1
70D	3.9±1.0	12.2±3.0	2.9
72D	4.3±1.1	13.9±3.5	2.7
76D	4.2±1.0	14.4±3.6	2.4
81D	3.1±0.8	11.1±2.8	2.1
84D	3.9±1.0	14.8±3.7	2.0
96D	4.3±0.9	18.5±3.7	1.5
106D	4.4±1.1	21.1±5.2	1.2

[a]Obtained by measuring the time development of the Rb^+-ion signal.

those determined using SFI. Thus it is possible to equate the rate constants measured for collisional depletion of the total excited-state population with those for collisional ionization.

The measured rate constants are listed in Table I and are plotted in Fig. 3 together with the results of earlier studies in this laboratory using Xe(nf) Rydberg atoms.[1] Also included are rate constants for Rydberg electron attachment calculated on the basis of the essentially-free-electron model using the expression

$$k = \int v\sigma(v)f(v)dv \ , \tag{4}$$

where $f(v)$ is the Rydberg electron velocity distribution and $\sigma(v)$ is the attachment cross section for *free* electrons.

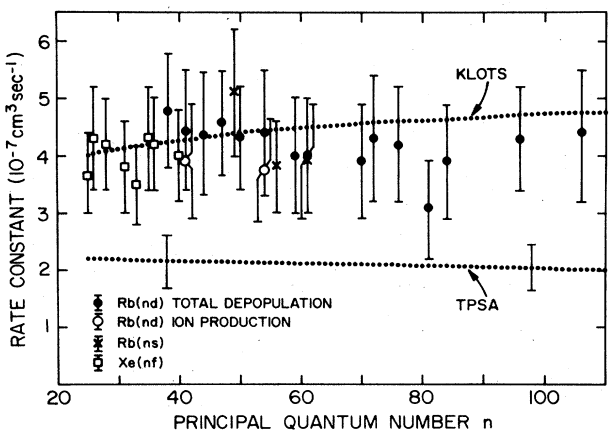

FIG. 3. Rate constants for collisional ionization in Rydberg-atom—SF_6 collisions. Rate constants derived using Eq. (4) and both the theoretical expression of Klots (Ref. 18) and the free-electron TPSA data (Ref. 9) are also included.

The rate constants calculated using the theoretical form for $\sigma(v)$ derived by Klots[18] assume an SF_6 polarizability α of 6.52 Å^3.[19] The second set of calculated rate constants were derived using an empirical expression for $\sigma(v)$ derived from measurements using the TPSA technique.[9]

The present data are in excellent agreement with the results of earlier studies[1] in this laboratory at lower n using Xe(nf) atoms. As Fig. 3 illustrates, the rate constant for collisional ionization is essentially independent of n and does not have a strong l dependence. The rate constant is thus independent of the Rydberg electron velocity distribution, implying that the cross section for Rydberg electron attachment to SF_6 is inversely proportional to the electron velocity.

Rate constants for Rydberg electron attachment derived using the theoretical expression of Klots are in excellent agreement with the present data. Rate constants derived using the recent TPSA free-electron data display the same n dependence as the present results but differ somewhat in absolute magnitude. However, the overall agreement between the present measurements and results predicted on the basis of free-electron data indicates that a Rydberg electron interacts with a target molecule much as does a free electron of equal kinetic energy. This parallel is further demonstrated by the fact that collisions with both free and Rydberg electrons result in the formation of the same negative ion species. The negative ions produced in the present work were identified using time-of-flight spectroscopy, for which purpose a small pulsed electric field was applied across the interaction region to drive the negative ions to the particle multiplier. As in free-electron studies,[7] the predominant negative-ion species observed was SF_6^-. Free-electron production was not observed, indicating that collisional ionization proceeds via negative-ion formation.

To provide further comparison with free-electron data, cross sections σ_e for Rydberg electron attachment were derived from the measured rate constants using the simple expression

$$\sigma_e = k/v_{\rm rms} , \tag{5}$$

where $v_{\rm rms}$ is the root-mean-square velocity of the Rydberg electron. The values of σ_e so obtained are included in Table I and are plotted in Fig. 4. The data are positioned on the electron-energy axis according to the average kinetic energy of the Rydberg electron, which is equal to its binding energy. Also included in Fig. 4 are values of σ_e derived from earlier measurements with Xe(nf) Rydberg atoms, free-electron attachment cross sections obtained using the swarm[8] and TPSA (Ref. 9) techniques, and the theoretical result of Klots. The agreement between free-electron and Rydberg data is again evident.

The collisional ionization data point to the correctness of the essentially-free-electron model. One assumption in the free-electron model, however, is that post-attachment interactions between the product positive and negative ions are so small as to be unimportant. To test this assumption, and to determine whether it might account for the discrepancy between the present data and the free-electron TPSA results, a number of kinematic studies were undertaken using Xe(nf) Rydberg atoms and the apparatus shown in Fig. 5. Xe($^3P_0$) metastable atoms contained in a collimated, thermal-energy beam are excited using the focused output of a nitrogen-laser-pumped dye laser to a selected nf state. Excitation occurs, in zero electric field and in the presence of SF_6, between two planar, parallel fine mesh grids. After a known interaction time ($\sim$2–5 μsec) the product Xe^+ ions are expelled from the interaction region by a small, pulsed electric field of 2 μsec duration that is insufficient to ionize the remaining Rydberg atoms. The ions then drift through a field-free region prior to detection by a position-sensitive detector (PSD). The total ion flight time to the detector is $\sim$45 μsec.

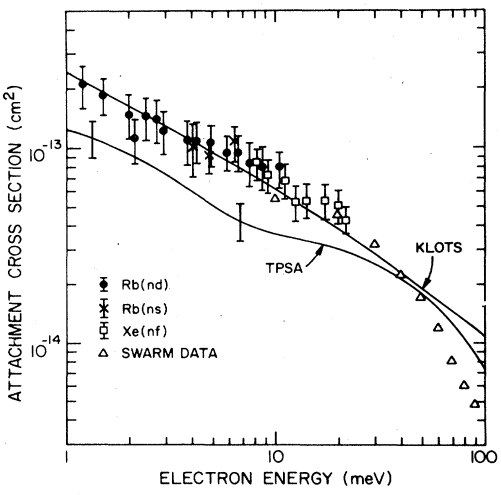

FIG. 4. Cross sections for Rydberg electron and free-electron attachment to SF_6. The solid lines show the theoretical result of Klots (Ref. 18) and the results of TPSA studies (Ref. 9).

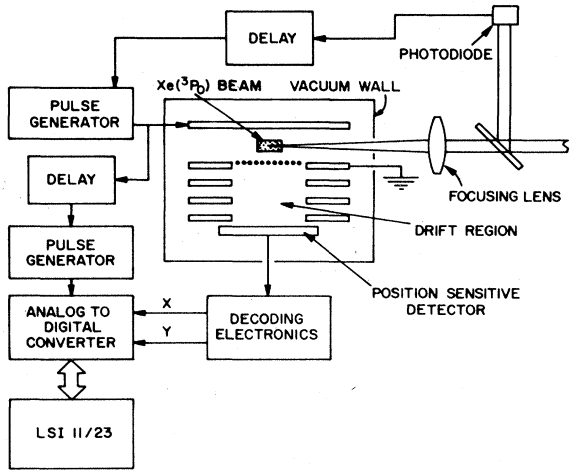

FIG. 5. Schematic diagram of the apparatus used to investigate the kinematics of Xe(nf)-SF_6 collisions.

Xe^+-ion spatial distributions at the detector are shown in Fig. 6 for several initial Rydberg states. Also included is the spatial distribution of Xe^+ ions produced by direct photoionization of the Xe($^3P_0$) atoms. Photoionization does not significantly change the trajectory of the ionized

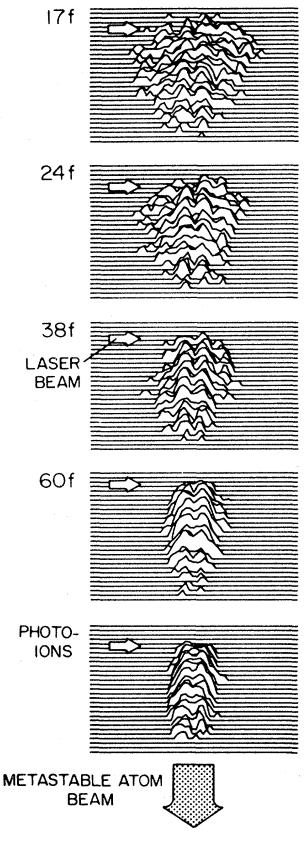

FIG. 6. Spatial distribution of Xe^+ ions at the PSD. The locations of the laser and metastable atom beams are indicated and the counts are plotted on a logarithmic scale.

atom. Thus the spatial distribution of Xe^+ photoions at the PSD will reflect the initial velocity distribution of photoexcited Rydberg atoms. Although the photoions are originally produced in a small volume, the velocity distribution of the atoms in the beam and the relatively long flight times to the detector lead to a substantial spread in arrival positions along the direction of the beam.

The spatial distribution of Xe^+ ions formed in $Xe(60f)$-SF_6 collisions is similar to that for Xe^+ photoions. The collisionally produced Xe^+ ions therefore must have a velocity distribution which is similar to that of the initial Rydberg atoms, demonstrating that there are no significant electrostatic interactions between the product Xe^+ and SF_6^- ions. This is expected because, at high n, the product ions will be formed at large separations. Given the long-range nature of Coulomb forces, other possible interactions must also be negligible. As n is decreased, however, the spatial distribution of the product Xe^+ ions broadens in the direction perpendicular to the beam axis. This shows that at low n, where the product ions are formed in closer proximity, electrostatic interactions do in fact change the trajectories of the product ions. Nevertheless, the data show that for values of $n > 40$ there is negligible interaction between the product ions, as assumed in the essentially-free-electron model.

In conclusion, the present data demonstrate that, for high n, Rydberg-atom collisions with targets that attach free low-energy electrons are well described by the essentially-free-electron model. Analysis of the data shows that the cross section for electron attachment to SF_6 at low energies ($\lesssim 10$ meV) is inversely proportional to the electron velocity v and, if v is expressed cm sec^{-1}, is given by

$$\sigma(v) = \frac{4.2 \pm 1.0}{v} \times 10^{-7} \text{ cm}^2 . \quad (6)$$

This research is supported by the National Science Foundation under Grant No. PHY84-05945 and the Robert A. Welch Foundation.

*Present address: Lincoln Laboratories, Massachusetts Institute of Technology, P.O. Box 73, Lexington, Massachusetts 02173.

[1]G. W. Foltz, C. J. Latimer, G. F. Hildebrandt, F. G. Kellert, K. A. Smith, W. P. West, F. B. Dunning, and R. F. Stebbings, J. Chem. Phys. **67**, 1352 (1977).

[2]G. F. Hildebrandt, F. G. Kellert, F. B. Dunning, K. A. Smith and R. F. Stebbings, J. Chem. Phys. **68**, 1349 (1978).

[3]I. Dimicoli and R. Botter, J. Chem. Phys. **74**, 2346 (1981); **74**, 2355 (1981).

[4]J. B. Astruc, R. Barbe, and J. P. Schermann, J. Phys. B **12**, L377 (1979).

[5]B. G. Zollars, K. A. Smith, and F. B. Dunning, J. Chem. Phys. **81**, 3158 (1984).

[6]For a discussion of this model see, for example, articles by M. Matsuzawa and by A. P. Hickman, R. E. Olson, and J. Pascale, in *Rydberg States of Atoms and Molecules,* edited by R. F. Stebbings and F. B. Dunning (Cambridge University Press, New York, 1983).

[7]For a review of low-energy electron attachment to molecules, see L. G. Christophorou, Adv. Electron. Electron Phys. **46**, 55 (1978).

[8]R. Y. Pai, L. G. Christophorou, and A. A. Christodoulides, J. Chem. Phys. **70**. 1169 (1979).

[9]A. Chutjian and S. H. Alajajian, Phys. Rev. A **31**, 2885 (1985).

[10]J. M. Ajello and A. Chutjian, J. Chem. Phys. **71**, 1079 (1979).

[11]S. Penselin, T. Moran, V. W. Cohen, and G. Winkler, Phys. Rev. **127**. 524 (1962).

[12]B. P. Stoicheff and E. Weinberger, in *Laser Spectroscopy,* edited by H. Walther (Springer, New York, 1979), Vol. IV, p. 264.

[13]C. J. Lorenzen and K. Niemax, Phys. Scr. **27**, 300 (1983).

[14]F. G. Kellert, T. H. Jeys, G. B. McMillian, K. A. Smith, F. B. Dunning. and R. F. Stebbings, Phys. Rev. A **23**, 1127 (1981).

[15]C. Higgs, K. A. Smith, G. B. McMillian, F. B. Dunning, and R. F. Stebbings, J. Phys. B **14**, L285 (1981).

[16]W. Walter, G. B. McMillian, K. A. Smith, and F. B. Dunning, Rev. Sci. Instrum. (to be published).

[17]F. G. Kellert, C. Higgs, K. A. Smith, G. F. Hildebrandt, F. B. Dunning, and R. F. Stebbings, J. Chem. Phys. **72**, 6312 (1980).

[18]C. E. Klots, Chem. Phys. Lett. **38**, 61 (1976).

[19]A. D. Buckingham and R. E. Raab, J. Chem. Soc. **23**, 5511 (1961).